

An Analysis of Dynamic Crack Initiation and Growth in Elastic-Viscoplastic Solids

G. RAVICHANDRAN

*Department of Applied Mechanics and Engineering Sciences,
University of California, San Diego, La Jolla,
California 92093, USA*

ABSTRACT

A numerical method for simulating dynamic crack initiation and growth under stress wave loading is described. Results are presented for both elastic and viscoplastic solids. Possible crack motions are considered and some insight is provided for crack growth criteria in elastic-viscoplastic solids.

KEYWORDS

Dynamic fracture; finite difference; elastic-viscoplastic

INTRODUCTION

In order to gain understanding of fracture processes in ductile solids under impact loading conditions, it is important to characterize the critical conditions that prevail near the vicinity of a dynamically growing crack. Analytical solutions are available for the problem of a semi-infinite crack in an infinite isotropic elastic body and results presented are crack-tip quantities, such as the history of the stress intensity factor $K_I(t)$; see Freund (1986). The results available for the rate dependent solids are limited and the analysis pertains to a dynamically growing crack under quasi-static far field loading conditions; see Brickstad (1983). Analytical solutions are in general not available for far-field quantities, such as particle velocities, and stresses for non-uniformly propagating cracks under stress wave loading conditions, which are essential for interpreting experimental measurements. Experimental techniques in dynamic fracture of opaque solids often rely on data obtained from far field measurements, such as particle velocities in a plate impact technique; see Ravichandran and Clifton (1986).

A finite difference method based on the work of Clifton (1967) is used in developing a numerical method for analyzing dynamic crack initiation and growth under stress wave loading conditions. A moving grid scheme is introduced for simulating dynamic crack growth. The numerical simulation is intended to model a plate impact dynamic fracture experiment where a plane, tensile square pulse of duration of about $1 \mu\text{s}$ impinges on a semi-infinite crack at normal incidence in a plate bounded by two free surfaces parallel to the crack plane. Details of the experimental

technique are described elsewhere; see Ravichandran and Clifton (1986). The accuracy of the numerical method is assessed by simulating crack initiation and growth in linearly elastic solids and comparing the results with available analytical results; Freund (1986). In the elastic-viscoplastic analysis some possible crack motions are considered and attempts are made to develop insight into critical conditions that prevail at a crack tip.

GOVERNING EQUATIONS

The equations governing the dynamic deformation of an isotropic elastic-viscoplastic solid under conditions of plane strain can be written in the non-dimensional form for small strains as

$$\begin{aligned} u_t - p_x - q_x - s_y &= 0 \\ v_t - p_y + q_y - s_x &= 0 \\ \left(\frac{\gamma^4}{3\gamma - 4}\right) p_t + \left(\frac{\gamma^2(2-\gamma^2)}{3\gamma - 4}\right) r_t - u_x - v_y &= -\frac{2}{3}D(p-r) \\ \gamma q_t - u_x + v_y &= -2qD \\ \gamma s_t - u_y - v_x &= -2sD \end{aligned} \quad (1)$$

and an evolutionary equation

$$\left(\frac{\gamma^2(2-\gamma^2)}{3\gamma - 4}\right) p_t + \left(\frac{\gamma^2(\gamma - 1)}{3\gamma - 4}\right) r_t = -\frac{2}{3}D(p-r) \quad (2)$$

where

$$D = \frac{\Phi(F)}{2\sqrt{J_2}} \quad (3)$$

Subscripts denote partial differentiation with respect to the subscript variable; u and v denote dimensionless particle velocities in the x and y directions respectively. $\Phi(F)$ is the viscoplastic shear strain rate in a simple shear experiment. The function F denotes the effective flow stress for an isotropic material; J_1 , J_2 , and J_3 are the invariants of the deviatoric stress tensor.

The dimensionless stress components p , q , r , and s are defined by

$$p = (\sigma_{xx} + \sigma_{yy})/2, \quad q = (\sigma_{xx} - \sigma_{yy})/2, \quad r = \sigma_{zz}, \quad s = \sigma_{xy}$$

σ_{xx} , σ_{yy} , σ_{zz} , and σ_{xy} are the dimensionless Cartesian stress components. Stresses have been normalized by ρc_L^2 , velocities by c_L , and time by b/c_L where ρ is the mass density, c_L is the longitudinal wave speed and b is a characteristic length in the problem that is being considered. In Eqn. (1)

$$\gamma = c_L/c_s \quad (4)$$

where c_s is the shear wave speed.

In terms of the dimensionless stress quantities p , q , r , and s the dimensionless second invariant of J_2 becomes

$$J_2 = \sqrt{\frac{1}{3}((p-r)^2 + 3(q^2 + s^2))} \quad (5)$$

NUMERICAL SCHEME

In case of isotropic linear elasticity, the function D is zero. In the absence of viscoplasticity, Eqn. (1) is recognized as a linear homogeneous symmetric hyperbolic system of first order partial differential equations with constant coefficients. The numerical solution to this system of equations is described by Clifton (1967). The finite difference equations are based on the method of integration along bi-characteristics. The difference scheme is an explicit single step method and the difference scheme is second order accurate. The domain of calculation is divided into a square mesh.

The interaction of a step pulse with a semi-infinite crack in a body bounded by two parallel surfaces is modelled as a mixed initial and boundary value problem. The domain of the calculation is shown in Fig. 1. The specimen thickness is normalized by the semi-thickness of the specimen, which is assumed to be the characteristic length b in the problem. The crack is located midway between the two bounding surfaces. The crack tip is located halfway across the specimen of width $2L$, which is taken to be sufficiently large to avoid unwanted reflected waves during the time of interest. The unit normalized time in the problem corresponds to the time a longitudinal wave takes to traverse the semi-thickness of the specimen.

A plane square tensile pulse of duration t_L and amplitude σ_0 is applied to the boundary $y=1$. The tensile pulse is applied by prescribing nodal normal stress values at the boundary $y=1$. The crack is located on the plane $y=0$ and $x<0$ with $x=0, y=0$ being the crack tip. The crack is represented by the two traction free surfaces $x<0, y=0^-$; and $x<0, y=0^+$.

Crack propagation is simulated by a moving grid scheme. As the crack propagates the entire mesh moves with the velocity of the crack. The instantaneous crack velocity is denoted by \dot{a} is prescribed. Since the crack position is known at every time step, the variables at the end of every

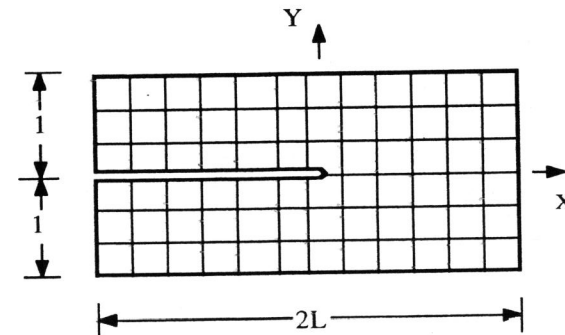


Fig. 1. Model geometry for computational analysis.

time step are interpolated to compute the variables at the nodal positions for the next time step. Now the computations using the difference method are continued, since we have the information as in the original computational scheme. Usually the mesh had 100 elements across a unit normalized distance and $L=1.5$ was used. A uniform Courant number of 0.5 was used in all calculations. All calculations were done for a Poisson's ratio of 0.3, which is the only material property that is needed as input once the problem is non-dimensionalized. The computations were carried out for a pulse duration of $t_L=1.4$. This pulse duration was chosen to correspond to a time duration of $1 \mu s$ step pulse used in the plate impact experiments; see Ravichandran and Clifton (1986). All the computations were carried out on a Cray X-MP.

The dynamic energy release rate G (Freund, 1986) for a two dimensional body containing a crack can be written as:

$$G = \lim_{\Gamma \rightarrow 0} \int_{\Gamma} [(U+T)n_x - \sigma_{ij}n_j u_{i,x}] d\Gamma \quad (6)$$

where U is the stress work density, T is the kinetic energy density, σ is the stress tensor, and \underline{u} is the displacement vector. Γ is a contour enclosing the crack tip and \underline{n} is the outward normal to the crack-tip contour (see Fig. 2). The energy release rate G was computed at the end of every time step using a domain integral form; see Li *et al.* (1986).

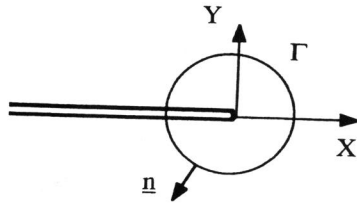


Fig. 2. Crack-tip contour for evaluation of dynamic energy release rate.

RESULTS

Linear Elastic Model

Results for specific examples of stress wave loaded cracks and comparisons with analytical results are presented in this section for linear elastic solids. The crack may move at either a constant velocity or at a nonuniform crack velocity. The analytical solutions for the stress intensity factor $K_I(t)$ and energy release rate G can be found in Freund (1986). The computed energy release rate provides a check on the accuracy and convergence of the numerical method used for this problem. Two different crack propagation models are considered, a constant energy release rate model, and a constant crack velocity model. Incubation time τ is the delay time for the onset of fracture, is the time when the virtual energy release rate reaches a critical value G_c .

We take $t=0$, to be the time of arrival of the plane wave on the crack plane. Figures 3 a and 3 b correspond to the constant energy release rate model and the constant crack velocity model for a delay time of $\tau=0.33$. In the case of the constant energy release rate model, the velocity-time history for the crack is shown as an insert in the plot. The crack remains stationary until time $t=\tau$.

At $t=\tau$ the crack begins to advance at zero velocity and accelerates to a maximum velocity at the end of the loading at $t=t_0$. In this case the energy release rate is to remain constant after the delay time. The numerical solution shows excellent agreement with the analytical solution when the crack is stationary. Once the crack begins to move the numerical solution oscillates about the analytical solution and the amplitude of the oscillations decay with time. In the case of the constant crack velocity model, the analytical solution predicts a jump in the value of energy release rate G at time τ , and thereafter the energy release rate grows linearly with increasing time. The numerical solution agrees well with the analytical solution, except immediately after the step at time τ . Here the numerical solution shows a smooth transition from the solution for a stationary crack to that of a moving crack. The crack velocities are normalized with respect to the Rayleigh wave speed, c_R . These results provide a check on the accuracy of the finite difference solution scheme used for simulating dynamic crack initiation and growth.

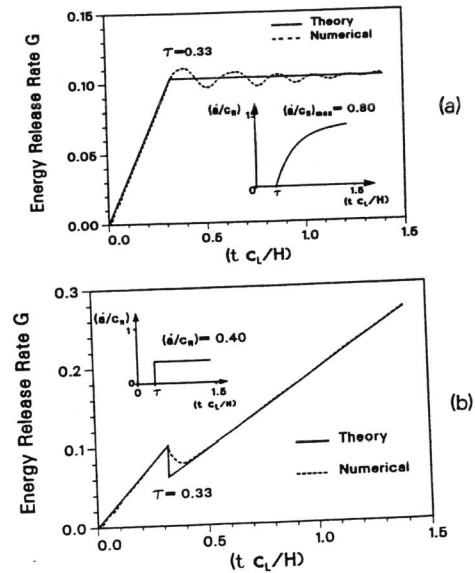


Fig. 3 Comparison of energy release rate from computational analysis with analytical solution; (a) constant energy release rate model, (b) constant crack velocity model.

Elastic-Viscoplastic Model

The numerical solution technique described earlier is modified for analyzing the problem of a step pulse impinging on a semi-infinite crack in an elastic-viscoplastic material bounded by two free surfaces. Possible crack-tip motions are examined in order to develop possible fracture criteria for dynamic crack growth in ductile materials.

Since the stresses at nodal points are unknown in the viscoplastic case, an iterative procedure must be used for solving Eqn. (1) using centered differences. Initial values for the stresses at a

nodal point at the current time step are taken to be the same as the stresses at that nodal point in the previous time step. The solution is computed using a single iteration at each mesh point. Crack propagation was simulated using the moving grid scheme described earlier.

The viscoplastic strain rate function that is used in the calculations was a function that models the strain rate sensitivity of many metals over quite a wide range of strain rates which is given by

$$\Phi(F) = \dot{\epsilon}_0 \exp(-2k_0/k) \quad (7)$$

$$k = \sqrt{J_2}$$

where k_0 is a reference shear stress and $\dot{\epsilon}_0$ is a reference shear rate. These constants are chosen by fitting experimental data. The strain rates ahead of the crack tip are estimated to be in excess of 10^5 s^{-1} where rate effects become important. A non-dimensional reference shear rate of $\dot{\epsilon}_0 = 6.666$ and a reference shear stress of $k_0 = 0.01$ were chosen to correspond to the material used in the plate impact experiments, namely 4340 VAR steel; see Ravichandran and Clifton (1986). The reference shear rate $\dot{\epsilon}_0$ was chosen to be 10^7 s^{-1} .

The impact pressure σ_0 was applied on the boundary of the specimen. Three distinct cases were considered with different impact pressures, incubation times, and crack velocities with normalized values, (i) $\sigma_0=0.004$, $\tau=0.85$, $\dot{a}/c_R=0.35$, (ii) $\sigma_0=0.005$, $\tau=0.5$, $\dot{a}/c_R=0.5$, and (iii) $\sigma_0=0.006$, $\tau=0.35$, $\dot{a}/c_R=0.5$. The incubation time τ and the crack velocity \dot{a} were chosen from correlation with experimentally measured crack growth given by Ravichandran and Clifton (1986). As in the elastic case the crack remained stationary until time τ and at τ the crack began to propagate at a prescribed constant velocity.

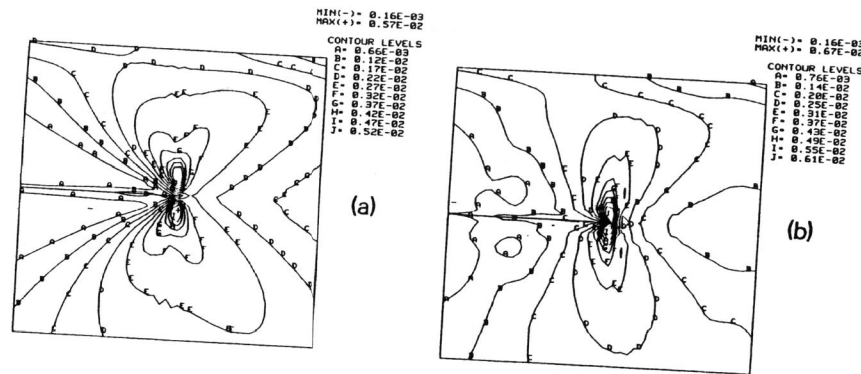


Fig. 4 Contours of effective stress at $t=1.4$; (a) Stationary crack, (b) constant velocity crack growth, $\tau=0.5$, $\dot{a}/c_R=0.5$.

In order to understand the evolution of a yield zone at the crack tip, constant effective stress contours (k) are shown in Fig. 4, for case (ii) at a normalized time of 1.4. Figures 4 a and 4 b correspond to when the crack is stationary, and when crack initiated at $\tau=0.5$ and propagated at 50 % of the Rayleigh wave speed. The normalized flow stress is 0.004 in these simulations. The

yield zones are nearly symmetric even though the loading is non-symmetric. In the case of the stationary crack (Fig. 4 a) the shapes of the contours are similar to the shape of the plastic zone under quasi-static loading. Also, it is interesting to note that the effective stress around the propagating crack (Fig. 4 b) is relatively higher than for the stationary crack. This implies that the plastic strains accumulate much more rapidly ahead of a propagating crack tip.

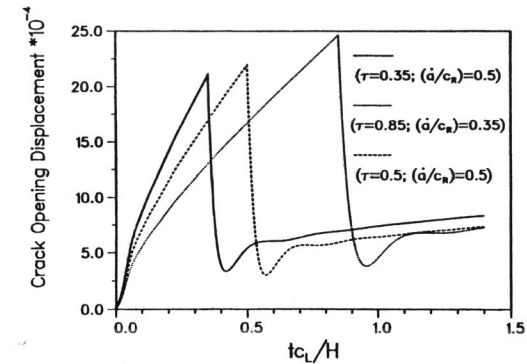


Fig. 5 Crack opening displacement (COD) as a function of time.

To gain better understanding of critical conditions that prevail near the crack tip, the crack opening displacement is plotted in Fig. 5. The plot shows that the crack opening displacement increases with time until the crack initiates and remains nearly constant during the constant velocity crack propagation. The crack opening is approximately the same for all the three cases during propagation. This suggests that a critical crack opening displacement might be a valid fracture criteria for constant velocity crack growth in elastic-viscoplastic solids under stress wave loading conditions.

Acknowledgement

The author is grateful to Professor R. J. Clifton of Brown University for suggesting this problem and for many helpful discussions. This research was supported by the Army Research Office through a grant to Brown University. Access to the CRAY at NCSA was made possible by a NSF grant to the Materials Research Laboratory at Brown University.

REFERENCES

- Brickstad, B. (1983) A Viscoplastic Analysis of Rapid Crack Propagation in Steel, *J. Mech. Phys. Solids*, **31**, p. 307.
- Clifton, R. J. (1967) A Difference Method for Plane Problems in Dynamic Elasticity, *Q. Appl. Math.*, **25**, p. 97.
- Freund, L. B. (1986) The Mechanics of Dynamic Fracture, *Proceedings of the Tenth National Congress on Theoretical and Applied Mechanics*, Austin, Texas.
- Li, F. Z., C. F. Shih and A. Needleman (1985) A comparison of Methods for Calculating the Energy Release Rate, *Engineering Fracture Mechanics*, **21**, p. 405.
- Ravichandran, G. and R. J. Clifton (1987) Dynamic Fracture Under Plane Wave Loading, *Brown University Technical Report*, Providence, Rhode Island (to appear in *Int. J. Fract.*).